Structural Analysis Methods for the Roll-Out Solar Array Flight Experiment

Matthew K. Chamberlain[1]
NASA Langley Research Center, Hampton VA 23681

Steven H. Kiefer[2]
Deployable Space Systems, Santa Barbara CA 93111

and

Jeremy A. Banik[3]
Air Force Research Laboratory, Space Vehicles Directorate, Kirtland AFB, NM 87117

The Roll-Out Solar Array (ROSA) flight experiment was launched to the International Space Station (ISS) on June 3rd, 2017. ROSA is an innovative, lightweight solar array with a flexible substrate that makes use of the stored strain energy in its composite structural members to provide deployment without the use of motors. This paper discusses the effort to model the structural dynamics of ROSA using finite element modeling. Two distinct and agnostic approaches were used by separate teams to assess the structural dynamics of the solar array prior to ground vibrational testing and flight testing. Results from each approach are compared to measured dynamics from accelerometers and photogrammetry data gathered on orbit. Advantages and disadvantages of each approach are discussed as are preliminary efforts to calibrate the models to the empirical data for the benefit of future modeling efforts on similar space structures.

Nomenclature

N	=	Membrane forces per unit width
M	=	Bending moments per unit width
A	=	Extensional laminate stiffness matrix
B	=	Coupling laminate stiffness matrix
D	=	Bending laminate stiffness matrix
ε^0	=	Laminate reference plane strains
κ	=	Laminate reference plane curvatures
ΔT	=	Change in temperature from the stress free temperature
M_{th}	=	Thermal-mechanical membrane forces per unit width
B_{th}	=	Thermal-mechanical bending moments per unit width
R_b	=	Slit-tube-boom radius

I. Introduction

The Roll-Out Solar Array (ROSA) is an innovative, lightweight solar array with a flexible substrate that makes use of the stored strain energy in its composite structural members to provide deployment without the use of motors. It has been developed in recent years by Deployable Space Systems, Inc. (DSS) with the support of the Air Force Research Laboratory (AFRL), the National Aeronautics and Space Administration (NASA) with the goal of providing space missions with more electrical power from a lighter structure that takes up less volume than conventional rigid panel arrays. AFRL and the Department of Defense Space Test Program led the development of a 4.67 meter long by 1.67 meter wide experimental ROSA wing that was launched to the International Space Station (ISS) on board a

---

[1] Research Aerospace Engineer, Structural Dynamics Branch, 4B West Taylor St, AIAA Senior Member
[2] Structural Analyst, 460 Ward Dr, AIAA Member
[3] Senior Research Engineer, 3550 Aberdeen Avenue SE, AIAA Associate Fellow

American Institute of Aeronautics and Astronautics

Falcon 9 Commercial Resupply Services mission (CRS-11) on June 3rd, 2017. After two weeks in space in the unpressurized trunk of the SpaceX Dragon spacecraft, the ROSA wing was the subject of a series of experiments to measure the functionality in the extreme temperatures and micro-gravity of orbital flight. Detailed descriptions of the ROSA experiment flight operations can be found in Refs. [1-9] while photogrammetry methods used during experimentation are discussed in Ref. [10]. The results of the on-orbit structural dynamics experiments were explored using accelerometer data in Ref [11] and are discussed in further depth with results derived from photogrammetry in Ref. [12]. This paper will focus on the details of the analysis models and methods developed to predict the on-orbit structural performance of the ROSA wing. Differences in the predictions will be discussed, as will differences between the predictions and the actual dynamics observed on orbit. Using the on-orbit results presented in Refs. [11-12], the models will be adjusted to improve their accuracy.

ROSA consists of a pair of longitudinally-oriented high-strain-composite slit tube booms attached at their tip to a mandrel and at their root to a yoke and spacecraft adapter (see Fig. 1). The Integrated Modular Blanket Assembly (IMBA) is tensioned between the spreader bar and root tube. It consists of lightweight photovoltaic power modules attached to mesh. For the flight experiment, the IMBA was only partially populated with six active strings of solar cells and was otherwise covered with similarly-shaped mass simulators. When rolled up on the mandrel to be stowed for launch (see Fig. 2), the composite slit tubes on ROSA provide the stored strain energy needed for deployment. This eliminates the need for a deployment motor reducing the part count and complexity of the overall solar array. For the flight experiment, ROSA was attached to a root structure containing instrumentation, cameras, and a linear actuator that was used to drive sinusoidal motion at the base of the solar array for the purpose of studying its dynamic characteristics. The whole experimental structure was attached to a Flight Releasable Attachment Mechanism (FRAM) which was used as an interface both to the Dragon capsule during launch and the ISS Special Purpose Dexterous Manipulator (SPDM) during experimentation.
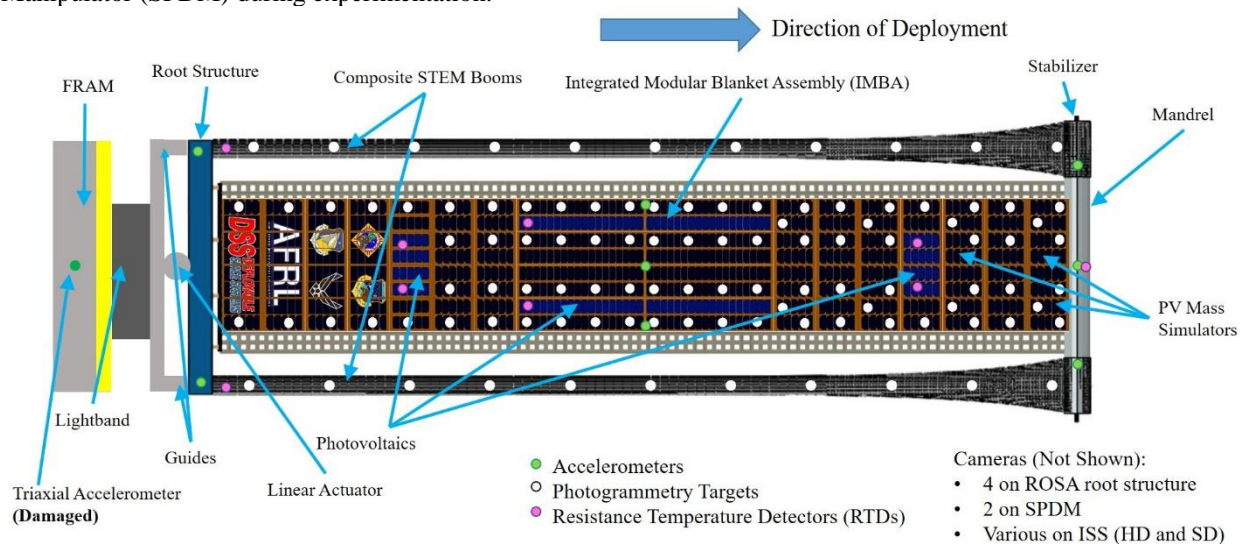

Fig. 1 Top-down view of ROSA flight experiment hardware

The embodiment of ROSA for the flight experiment presents some unique analysis challenges. In a typical ROSA configuration, the high-strain composite slit tube booms are allowed to deploy until they return to their original cylindrical cross section all along their length. In order to allow for retraction after experimentation, the flight experiment array's booms were not fully closed at their tips. Instead, their tips remained flattened to the mandrel on the outboard end of the array throughout experimentation. The partially closed booms develop transition zones between the fully formed circular sections and the partially rolled sections remaining on the mandrel. The prediction and incorporation of the boom transition zone into the dynamic models is important for capturing the potential impacts these transition zones have on the deployed structural performance of the ROSA wing. In addition, the Integrated Modular Blanket Assembly (IMBA) is a tensioned flex blanket, deriving the vast majority of its stiffness from tension applied by a mechanical system in the array. The IMBA is constructed of a light-weight tensioned, orthogonal open-weave backplane on which the relatively heavy photovoltaic components and associated harnessing are mounted. Capturing the IMBA's tensioned stiffness is critical to accurately modeling the ROSA dynamics performance.
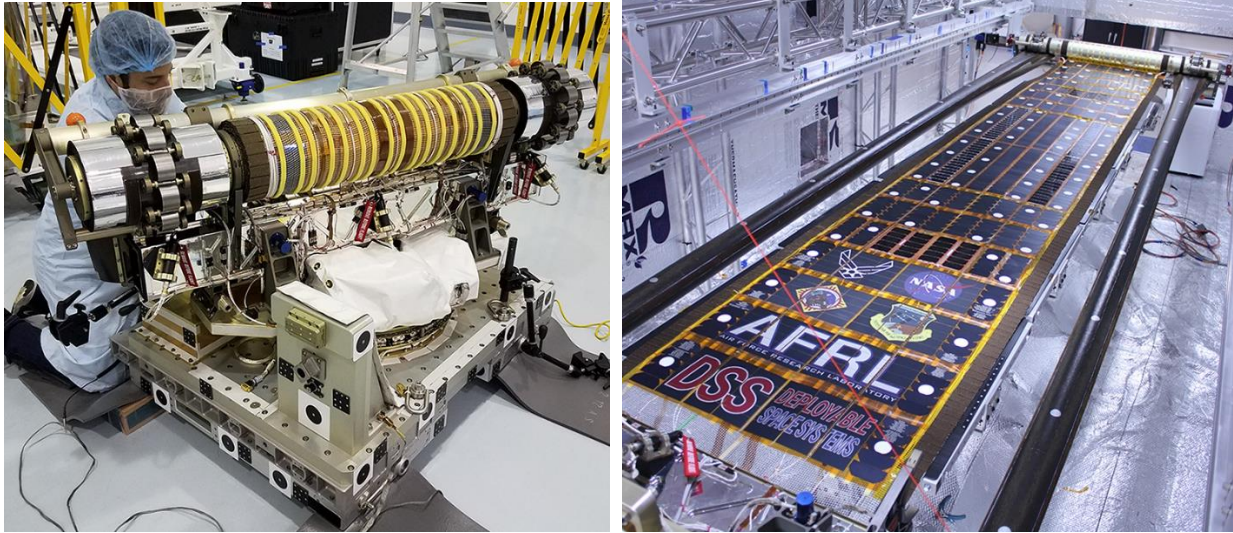
American Institute of Aeronautics and Astronautics

Fig. 2 layout of the ISS ROSA flight experiment wing stowed (left) and deployed (right) during ground testing

The unique features of the ROSA design were captured in two independently developed analysis models using different techniques for each modeling challenge and slightly different assumptions. One model was developed by a government team using the Abaqus analysis software package and using nominal material properties based on manufacturer specifications. The other was developed by DSS using the Ansys analysis software package. Where possible, the Ansys model made use of material properties based on mechanical tests. The other key differences between the models, as summarized in Table 1, are in the modeling of the slit tubes and the IMBA but there are numerous other small differences throughout. Each approach has its advantages and disadvantages, as will be discussed throughout this paper. The focus of this paper is on the two modeling techniques, how well they did in predicting ground test and flight test results, and how changes in the models might better predict the performance of future ROSA designs

Table 1 Summary of finite element modeling approaches

	Government Model	Deployable Space Systems Model
Software Used	Abaqus Standard and Explicit	Ansys
Slit Tube Transition Zone Modeling	Explicit model of flattening and rolling of boom onto mandrel.	Pre-integrated shell section model with applied thermal loads
Integrated Modular Blanket Assembly Modeling	Mesh of scaled beams with nonstructural mass	Effective shell method
Material Properties	Based on nominal manufacturer specifications	Based on measured values where possible

II.   Modeling Methods

The two key aspects of ROSA are the composite slit tubes that provide both the primary structural members and means of deployment and the IMBA blanket which contains the photovoltaics. The modeling of each of these key sub-structures by the two teams is described here, as is the process of integrating the whole model.

A. Slit-Tube Modeling

The high-strain composite slit-tube-booms provide the motive force for deployment and become the backbone of the structure when deployed. The booms are manufactured in their deployed state on a cylindrical mandrel. In their stowed state, the booms are reverse-rolled onto the mandrel, developing stored strain energy that is released during deployment. In a typical ROSA design, the fully unrestrained slit tube boom has a circular cross-section with a small gap at the slit when deployment is complete. In the ROSA flight experiment design, the very tip of the boom is kept flattened onto the mandrel even when the wing is fully deployed (see Fig. 3). This allows for retraction and re-stow for disposal in the Dragon trunk but it also creates a transition region in the boom that is more complicated to model than if the boom were allowed to return to the deployed state in which it was manufactured.

American Institute of Aeronautics and Astronautics

| **a.)** | Boom test article | **b.)** | ROSA flight experimet wing partially deployed |

Fig. 3 Slit tube boom transition zone

1. Explicit-to-Implicit Method (Abaqus)

The explicit-to-implicit method for developing the slit tube boom transitions involved the deformation of circular cross-section slit tubes by a rigid mandrel. A model of the nominal slit-tube with material properties taken from manufacturer specifications was built in Abaqus. One end of the boom was first flattened in an analysis step so that one of its ends could be constrained to a rigid mandrel. In order to flatten the boom, lateral forces and outward moments were applied to the edge of the boom's slit. The mandrel was then rolled over a specific portion of the boom with accurate stiffness properties but very little density, wrapping the enough of the boom up to achieve the desired deployed length (see Fig. 4). After rolling up the desired amount, the whole structure was allowed to relax. The large deformation and complex contact involved in these steps lent itself to explicit time integration analysis. The deformed shape was then imported into an implicit model that contained the rest of the ROSA system including the IMBA, stabilizer bar, spreader bar, blanket tension springs, and root tube. The implicit model was used for modal and harmonic analysis.
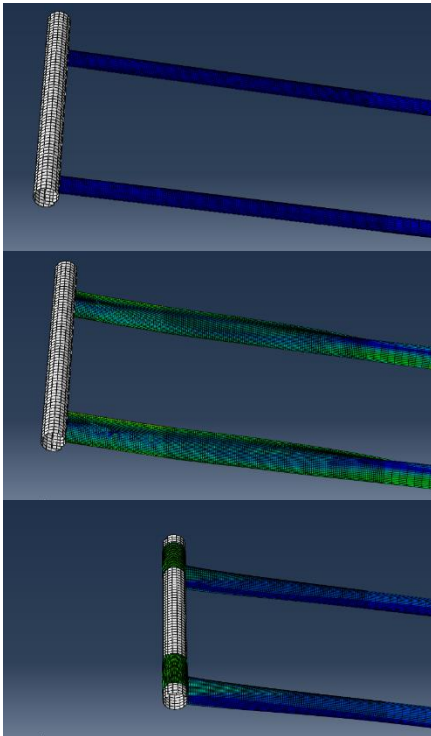
a.) Modeling of boom transition region in Abaqus Explicit
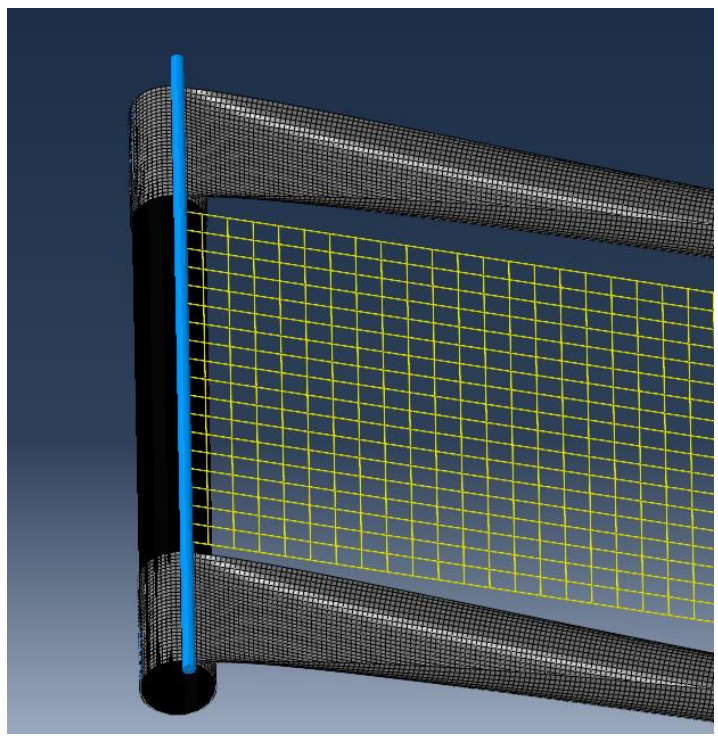
b.) Integration of flattened and rolled boom into ROSA assembly in Abaqus Standard

Fig. 4 Modeling of slit tube transition region in Abaqus

4

American Institute of Aeronautics and Astronautics

2. Pre-Integrated Shell Section Method (Ansys)

The pre-integrated shell section method was developed as an all-implicit analysis methodology. The pre-integrated shell stiffness properties are the A, B, D laminate stiffness matrices found in classical lamination theory (Eq 1, Ref. [13]). In Ansys membrane & bending thermal effects are also included (Eq 2) where *th* designates thermal force & bending resultants. Assuming a balanced and symmetric laminate ($B = 0$), and ignoring small bending twisting coupling terms, the equivalent running loads are computed for an applied curvature in the lateral direction equal to the boom radius (Eq 3). These running loads are the loads required to completely flatten a boom. The thermal force and bending moment terms can then be chosen such that an application of a change in temperature equal to the curvature of the boom generates internal forces and moments equal to those during the flattening of the boom (Eq. 4).

$$\begin{bmatrix} N \\ M \end{bmatrix} = \begin{bmatrix} A & B \\ B & D \end{bmatrix} \cdot \begin{bmatrix} \epsilon^0 \\ \kappa \end{bmatrix} \tag{1}$$

$$\begin{bmatrix} N \\ M \end{bmatrix}_{th} = \Delta T \cdot \begin{bmatrix} M_{th} \\ B_{th} \end{bmatrix} \tag{2}$$

$$\begin{bmatrix} N_x \\ N_y \\ N_s \\ M_x \\ M_y \\ M_s \end{bmatrix} = \begin{bmatrix} A_{xx} & A_{xy} & & & & \\ A_{yx} & A_{yy} & & & & \\ & & A_{ss} & & & \\ & & & D_{xx} & D_{xy} & \\ & & & D_{yx} & D_{yy} & \\ & & & & & D_{ss} \end{bmatrix} \cdot \begin{bmatrix} \\ \\ \\ \frac{1}{R_b} \\ \\ \end{bmatrix} = \begin{bmatrix} 0 \\ 0 \\ 0 \\ \frac{D_{xy}}{R_b} \\ \frac{D_{yy}}{R_b} \\ 0 \end{bmatrix} \tag{3}$$

$$[M_{th}] = [0], [B_{th}] = \begin{bmatrix} D_{xy} \\ D_{yy} \\ 0 \end{bmatrix}, \Delta T = (1/R_b) \tag{4}$$

The booms are modeled as flat sections with appropriate boundary conditions at the root and tip. A temperature load equal to the inverse of the boom radius is applied only to the boom sections. A geometric non-linear analysis is performed to capture the large deformations as the booms deform from flat to their final pre-stressed condition. Without any boundary conditions, the booms would deform to the radius of the boom but with the appropriate boundary conditions, the transition region in the partially-deployed ROSA for the flight experiment can be created. Examples of the application of this method in Ansys implicit pre-integrated section analysis to a free boom section and a boom section with the tip restrained are illustrated in Fig. 5. This method was used to model the fully-deployed ROSA booms with their transition zone for integration into the model of the rest of the array.
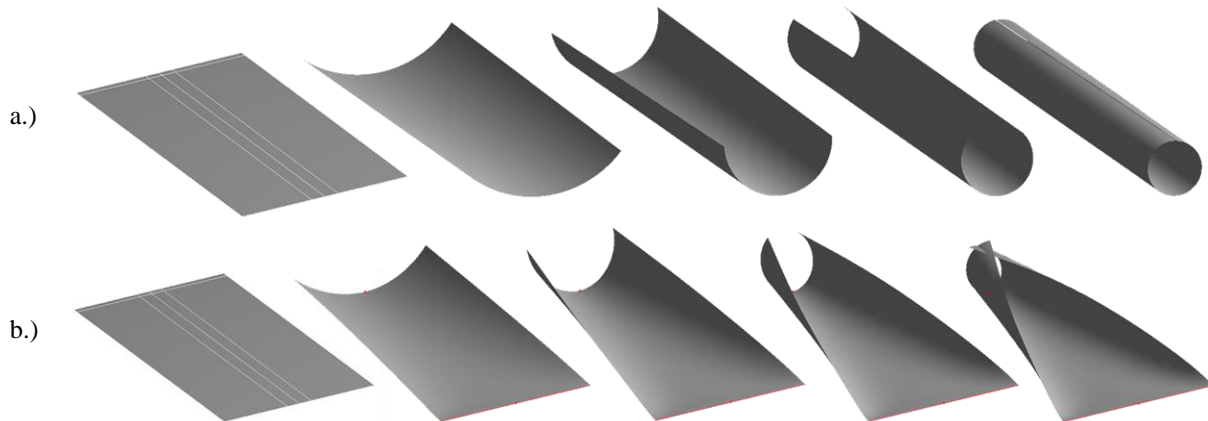

Fig. 5 Examples of free-deformation of a.) a slit tube boom (above) and b.) a tip-restrained slit tube

5

B. Tensioned IMBA Modeling

The Integrated Modular Blanket Assembly (IMBA) is the second key structural element of ROSA which was treated differently in the two finite element models. The IMBA (see Fig. 6) consists of lightweight photovoltaic power modules and their associated electrical harnesses attached to mesh. Despite the use of lightweight materials, IMBA accounts for a significant portion of the overall mass of ROSA. For launch, it is rolled up on the mandrel in between the two composite slit tubes. When fully deployed, it is tensioned using finely-tuned constant-force springs that attach to a thin stiffening strip that holds the end of the mesh. For the ROSA flight experiment, four tension springs were used between the IMBA and the root structure.
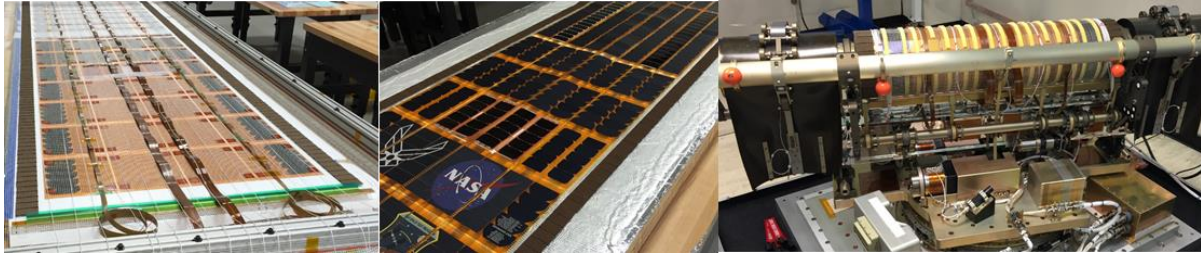

Fig. 6 IMBA mesh backplane (left), SPMs (center), & motor-actuated blanket tensioner (right)

3. Scaled Beam Mesh Method (Abaqus)

In an attempt to make a simple model of IMBA in Abaqus, a mesh of beam elements was modeled to capture the load transfer and tension distribution within the backplane (see Fig. 7). In order to reduce model size, the mesh was scaled to a 2in x 2in beam spacing which is roughly four times the actual mesh spacing. The cross sections of the beams were modeled as square and were scaled to match the measured areal density of the IMBA mesh assuming S-glass properties. Non-structural mass was added to the beam mesh to account for the actual mass of the materials attached to the mesh including photovoltaics, wiring, and foam attached to the back of the mesh for protection during storage among other things.
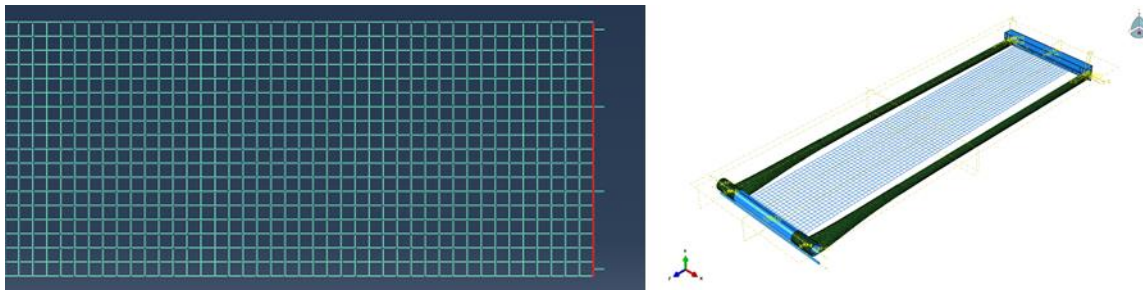

Fig. 7 Scaled beam mesh model of IMBA (left) integrated into the Abaqus model (right)

4. Effective Shell Method (Ansys)

The effective bending stiffness is the critical parameter in defining the structural dynamic behavior of the IMBA . For the Ansys model, the effective, un-tensioned stiffness was found using a test of an engineering development unit (EDU) IMBA blanket as shown in Fig. 8. A representative section of the blanket was allowed to form a catenary between two tables, one of which held a load cell. The amount of vertical sag was measured for various spans and tensions. These values were compared to a catenary model. The difference between the catenary model and observed measurements was converted to an effective stiffness. As expected, the computed effective stiffness of the IMBA was very low compared to the tensioned stiffness.

The final shell representation of the IMBA blanket utilizing the measured effective bending stiffness was included in the Ansys model as shown in Fig. 9. The in-plane extensional stiffness was modeled as a stiffness per width equivalent to S-glass rods of 0.010 inch diameter with a 0.25 inch x 0.25 inch spacing. A low value (100 psi) was assumed for the in-plane shear stiffness of the shell representation of the IMBA. As with the simplified Abaqus mesh model, non-structural mass was added to the shell model to account for the SPMs, harness, foam, etc.
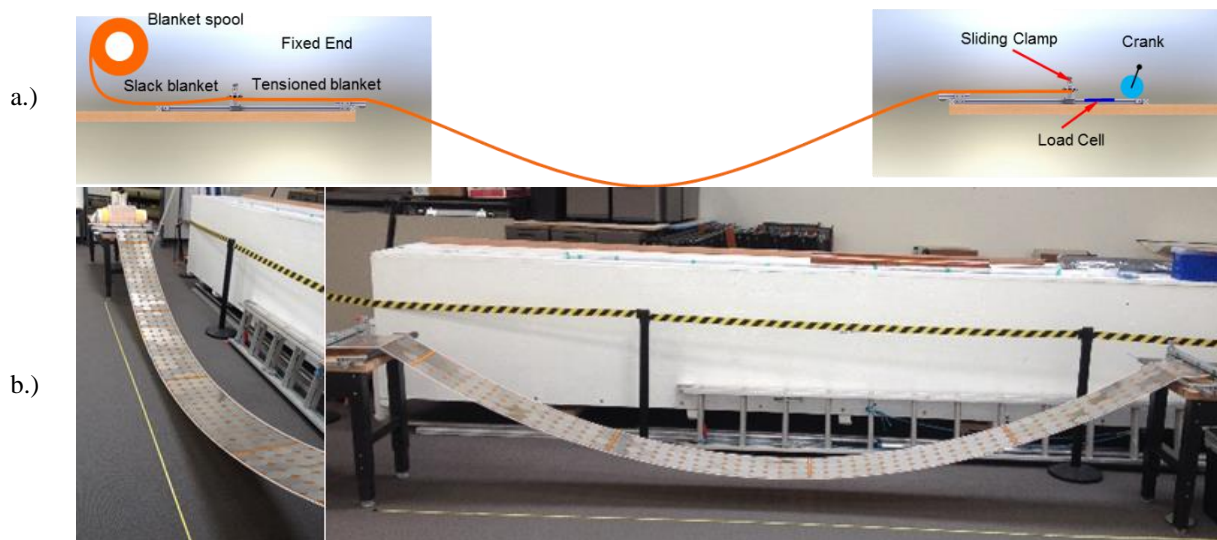
American Institute of Aeronautics and Astronautics

Fig. 8 IMBA effective bending stiffness test setup a.) Illustration and b.) Hardware test
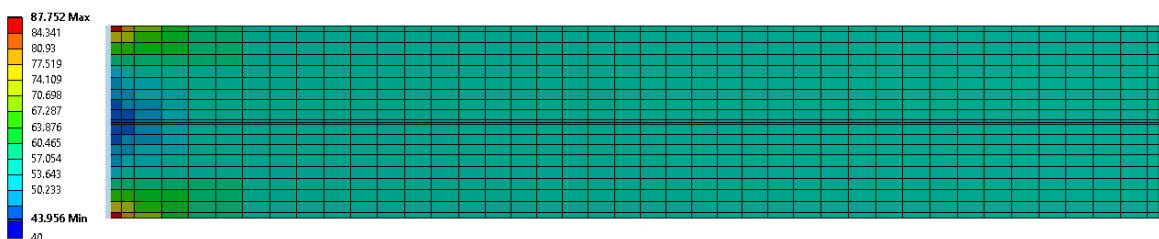

Fig. 9 Tension field in the effective shell model of IMBA employed in the Ansys FEM

C. Integrated Finite Element System Models

The slit tube boom and IMBA models discussed in previous sections were just two parts of larger models built to represent the ROSA flight experiment. After building up models of those two components as explained above, they were integrated into assemblies for final analysis of ROSA. The manner in which this was accomplished by each team is described here.

5. Integrated Abaqus System Model

The assembled Abaqus Standard model was built around the deformed booms modeled in Abaqus Explicit and imported as a set of geometry and material properties. Flexible beam and shell finite element representations of the mandrel, stabilizer, and root structure were added to the appropriate locations on the booms. The IMBA was tied to the mandrel and connected to the root structure through four bolt elements each with a stiffness similar to the constant force springs in the real mechanism. Prior to modal analysis, the bolt elements were pre-tensioned in a static step with one quarter of the total nominal blanket tension each to make the IMBA taught. The bolt elements were then locked at their pre-tension level in another static step before calculating modes and mode shapes. The complete ROSA assembly in Abaqus is shown in Fig. 10.
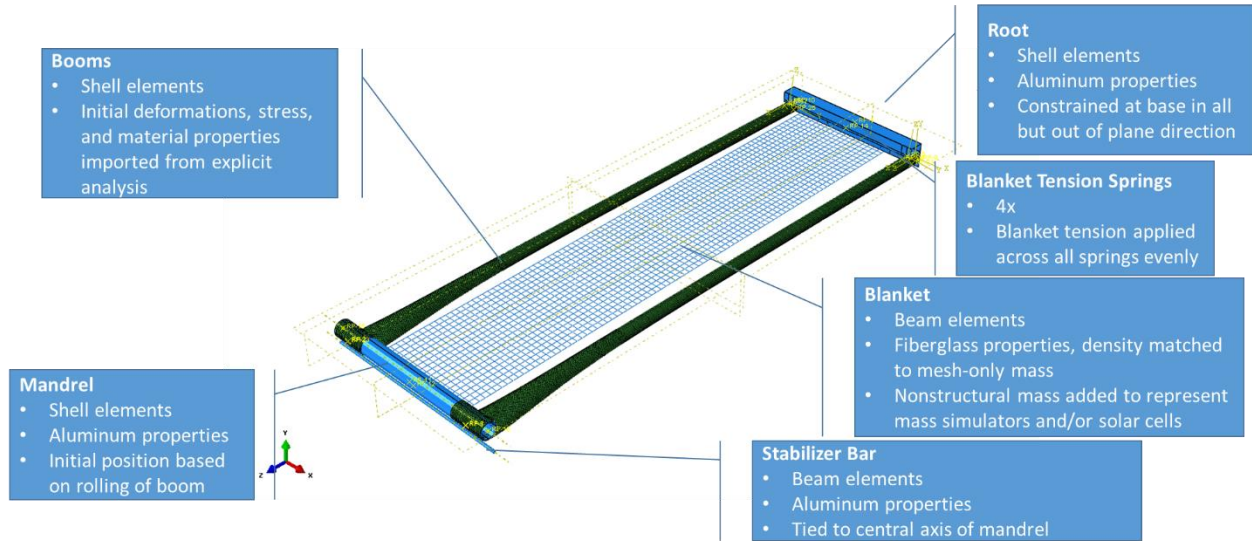
American Institute of Aeronautics and Astronautics

Fig. 10 Integrated Abaqus finite element model

6. Integrated ANSYS System Model

The integrated Ansys system model (see Fig. 11) included detailed representations of the mandrel and other tip hardware, root hardware, and a more accurate baseplate assembly model than did the Abaqus model. Each of these subsystems was comprised primarily of shell & beam elements with some springs at interfaces between components where required.
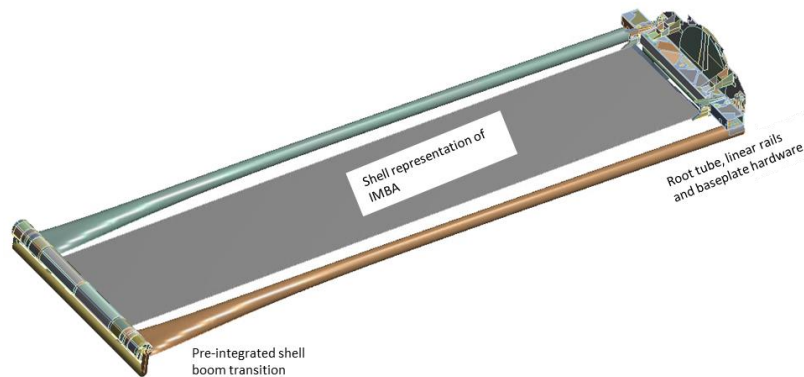

Fig. 11 Integrated Ansys finite element model

III.   Ground Test Dynamics Predictions & Analysis Comparisons

The dynamics of ROSA were explored prior to flight in a series of ground dynamics tests. A flight-like engineering development unit (EDU) of ROSA was constructed and hung vertically inside a thermal vacuum chamber as shown in Fig. 11. While the structure was offloaded for testing, the flexible blanket is very difficult to offload without interfering with the dynamics of the system. For this reason, two different substitute blankets were used during testing in place of an IMBA with working photovoltaics: the mesh by itself and mesh with mass and stiffness simulators added in place of solar cells. The mesh version of the blanket was given the nominal tension planned for use in flight while the stiffness simulator version of the blanket had lower applied tension to compensate for the gravity load created by its extra mass. The total tension experienced at the root was thus the same for both configurations.

The dynamics of the array were tested using the same linear actuator system planned for use in flight, providing a way of exercising the methods that would be used later on the ISS. Using the linear actuator, sinusoidal out of plane base motion was created with varying amplitude, frequency, and duration. Broad sine sweeps were used to identify system modes before more narrowly-concentrated sweeps were used repeatedly to verify the exact frequencies of the

American Institute of Aeronautics and Astronautics

first few modes. The EDU was instrumented in the same way as the flight unit, with three accelerometers on the mandrel, three in the middle of the blanket, and two at the roots of the slit tubes.
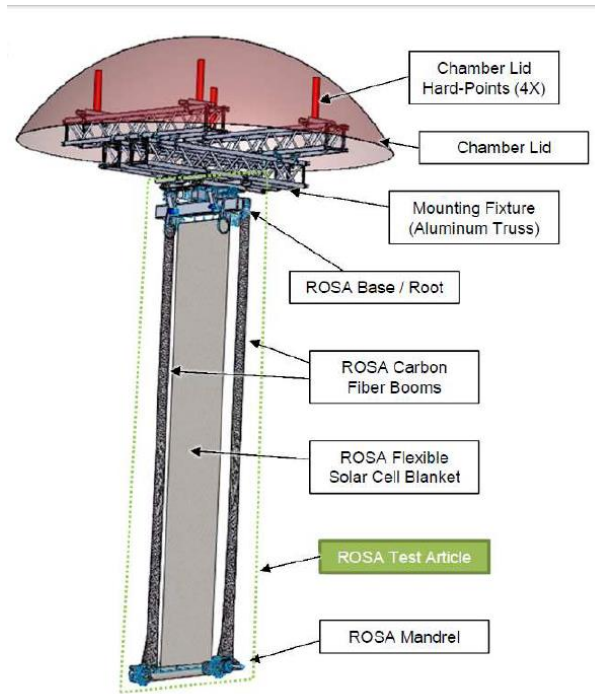

Fig. 12 Ground dynamics test configuration

Both modeling approaches were used to predict the modes and mode shapes of the EDU in the testing configuration as well as the accelerations that could be expected using each type of IMBA blanket substitute. These predictions are shown along with experimental results for the mesh blanket configuration in Table 2 and for the stiffness simulator configuration in Table 3. The dynamics of the EDU were consistent throughout testing, however the blanket edge mode seen during testing with the blanket that was only mesh did not show up when the blanket with stiffness simulators was used. The first structural mode was over-predicted by both methods, perhaps as a result of material models that were more stiff than the as-built structure and blanket tension that was modeled at a slightly higher value than was present in testing.

Table 2 Measured mesh-only EDU modes vs FEM predictions

Mode	Measured Frequency (Hz)	Abaqus Pre-Test FEM Prediction (Hz)	Ansys Pre-Test FEM Prediction (Hz)
Primary Structural	0.479	0.613	0.566
Blanket Edges	1.422	n/a	2.472
Blanket Center	2.356	2.149	2.083

Table 3 Measured stiffness simulator EDU modes vs FEM predictions

Mode	Measured Frequency (Hz)	Abaqus Pre-Test FEM Prediction (Hz)	Ansys Pre-Test FEM Prediction (Hz)
Primary Structural	0.484	0.601	0.554
Primary Blanket	1.17	1.490	1.263

Damping was calculated based on the free decay of various modes after excitation. For the EDU configuration in which the blanket was represented by mesh only, the average measured damping for the first structural mode was 3.2 % while the first blanket mode had an average measured damping of 1.5 %. For the stiffness simulator configuration,

9

American Institute of Aeronautics and Astronautics

the average measured damping for the first structural mode was 2.89 % on average for the first structural mode while it was 2.87 % for the primary blanket mode and 1.76 % for the secondary blanket mode.

The major lessons from the ground dynamics testing were that the finite element models may slightly over-predict the structural modes. The EDU dynamics were consistent throughout testing and were easily excited using the linear actuator at the root, allowing for a good dress rehearsal for flight operations on the ISS.

IV.   Flight Dynamics Predictions, Observations, and Analyses

Finite element models of the flight configuration were prepared in a manner similar to that which was used for the ground dynamics. The more flight-like IMBA blanket properties discussed in Section II B were utilized and the mass of various components added back into the models. The frequencies and mode shapes predicted by each model are summarized in Table 4 while some of the shapes are shown in Fig. 13. One key difference seen in these predictions is that the shell-based IMBA representation used in the Ansys model predicted many more complex blanket modes below 2 Hz (the planned cutoff for experimentation). The mesh-based Abaqus model was limited to what are essentially string modes for the blanket. For the primary structural modes and the blanket drum mode, however, the models made very similar predictions.

Table 4 Summary of ROSA modes and mode shapes from finite element models

Abaqus Model			ANSYS Model		
Mode	Frequency (Hz)	Shape	Mode	Frequency (Hz)	Shape
1	0.50	Structural Bending	1	0.54	Structural Bending
2	0.64	Structural Torsion	2	0.66	Structural Torsion
3	0.98	Blanket Drum	3	0.91	Blanket Torsion
4	1.24	Blanket Torsion	4	0.93	Blanket Saddle
5	1.88	2nd Order Blanket Drum	5	0.94	Blanket Drum
6	2.22	Lead-Lag in Plane	6	1.12	2nd Order Lateral Blanket Drum
			7	1.49	3rd Order Lateral Blanket Drum
			8	1.78	2nd Order Blanket Twist
			9	1.79	2nd Order Blanket Drum
			10	1.82	2nd Order Blanket Saddle
			11	1.87	Lead-Lag in Plane
			12	2.00	3rd Order Blanket Twist
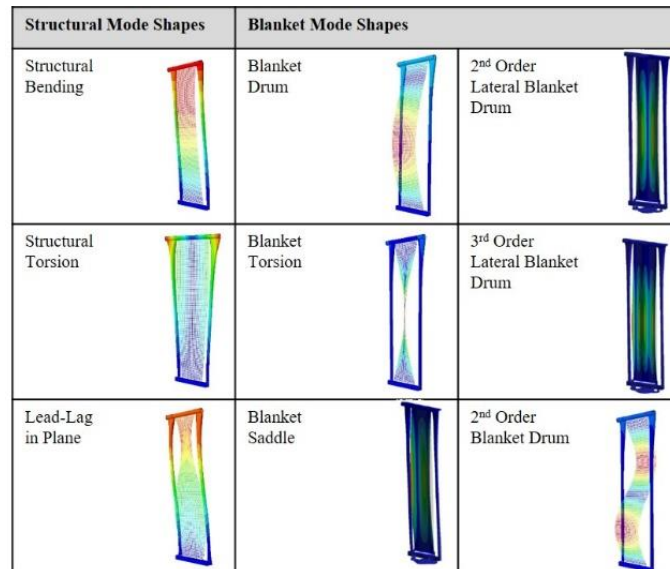
Fig. 13 Summary of ROSA FEM modes and mode shapes from both models

American Institute of Aeronautics and Astronautics

In addition to modeling the nominal configuration of ROSA prior to flight, a sensitivity study was carried out to explore how variations in the expected features and performance of the system could impact the structural modes. A number of factors were varied to create a select set of extreme worst-case scenarios in which the structural modes were either much higher or lower than expected. These extreme scenarios were meant to inform flight operations should initial sine sweeps reveal that the system modes were not where they were expected. The factors adjusted in the sensitivity study were all allowed to vary +/- 50% from their nominal value and included:

- Boom stiffness matrices, in which individual terms were allowed to vary;
- Boom slit width, which was allowed to vary while still maintaining the same amount of material in the boom cross section; and
- Blanket tension, which was still given a uniform distribution across the array.

Boom stiffness and the slit width were varied in an attempt to assess the effects of potential creep in the high-strain composite over months of storage and a week of orbiting the earth. After creep, it was judged possible that the boom could be stiffer or softer than expected and might not return to the same shape it had when manufactured and tested on earth.

While not meant to be exhaustive, the sensitivity study showed some clear trends. The blanket modes in general were far more sensitive to changes in factors, particularly blanket tension. When the blanket tension was low, certain combinations of other factors could lead the higher-order blanket modes to combine with one another or with the in-plane structural bending mode to create complex repeated modes. The order of modes was also changed in these situations. The slit width had very little effect on blanket modes at all and by itself only raised the first structural mode by 4% when it was 50% smaller than expected. The results of the sensitivity study are summarized in Table 5.

Table 5 Pre-flight sensitivity study results

Mode	Worst-Case Decrease in Frequency	Worst Case Increase in Frequency
Structural Bending	11%	8%
Structural Twist	9%	4%
Blanket Bending	33%	35%

The nominal element model predictions were used for the planning of flight operations. After a series of roughly three sine sweeps to verify the rough locations of the first structural mode and the key blanket modes a series of five narrower day and night sine sweeps were planned to be run around three key frequency ranges:

- The first structural mode (around 0.5 Hz)
- The structural twist mode and first few blanket modes (0.5 to 1.25 Hz)
- Higher order blanket modes (1.5 to 2.0 Hz)

As is explained in the next section, the plans based on the pre-flight finite element models had to be abandoned due to unexpected phenomena but the existing models still remained useful.

A. Unexpected On-Orbit Dynamics

Two unexpected phenomena were observed during the flight testing of ROSA (see Refs. [11-12]). First, in complete opposition to the trends seen in ground test results, the fundamental system bending mode was hard to excite in space and seemed to be highly damped. The first mode was also found to be 20% lower than was predicted by finite element models. After further analysis of both the ROSA data, space station cameras, and the SPDM joint torque data, it was hypothesized that the wing was imparting small amplitude vibrations back into the arm at the same frequency as the forced motion. This hypothesis could not be easily verified because a triaxial accelerator located on the FRAM was damaged and the photogrammetry targets located on the FRAM turned out to be hard to observe.

A second unexpected observation was that the right edge of the IMBA blanket seemed to vibrate at greater amplitude and lower frequency than the left edge. At low frequencies, the right edge seemed to have its own mode shape. At higher frequencies, the blanket modes seemed to be split into two parts: one involving the right edge and another in which the center and left edge of the blanket were excited. During flight operations, quick interrogation of the pre-flight models showed that discrepancies in blanket tension could be to blame for the splitting of the blanket edge modes. The reason for this behavior will be one of the focuses of post-flight model correlation.

B. Modal Analyses of Structural Dynamics Data

In previous work [11], accelerometer data was post-processed and analyzed using two methods in an attempt to identify the ROSA system modes, mode shapes, and damping. Data that was originally recorded at a rate of 200 Hz on the ISS was downlinked and filtered in various ways to help isolate system modes by identifying the peaks in the

American Institute of Aeronautics and Astronautics

Fast Fourier Transform (FFT) of the responses. Damping and approximate mode shapes were also using various methods. After aggregating the results from dozens of experiments, eight likely modes were identified below 2 Hz, as shown in Table 6.

In an accompanying paper [12], photogrammetry data from video recorded during select experimental runs was analyzed and found to be in good agreement with the accelerometer data analyzed previously (see Table 6). In addition, a number of blanket mode shapes were reconstructed in greater detail as shown in Table 7. The photogrammetry data showed in even more stark detail how the right and left blanket edge modes were separated into two right modes at about 0.61 Hz and 0.66 Hz and a left mode at about 0.78 Hz. The structural twist mode seemed to be mixed up with one or both of the right blanket edge modes.

Table 6   Summary of Structural Modes of ROSA (See Refs. [11-12])

System Mode	Based on Accelerometer Data		Based on Photogrammetry Data		Damping [%]
	Frequency [Hz]	Previously Assumed Mode Shape	Frequency [Hz]	Confirmed Mode Shape	
1	0.41	1st structural bending	0.39	1st structural bending "diving board"	3.50
2	0.60	Blanket right edge w/ torsion	0.61	1st structural torsion and right blanket edge flap	3.90
3	0.66	Blanket right edge w/ torsion	0.66	1st structural torsion and right blanket edge flap	1.60
4	0.81	Blanket left edge and center	0.78	Left blanket edge flapping	1.70
5	0.91 *	Blanket drum/saddle (day)	0.89 *	1st blanket drum/saddle (day)	0.85
6	1.18 *	Blanket drum/saddle (night)	1.14 *	1st blanket drum/saddle (night)	1.55
7	1.71	Blanket right edge	1.64	3rd order right blanket edge flap	0.70
8	1.80	Blanket right edge	1.83	2nd order blanket drum/saddle	1.05

Table 7   Separate left/right low frequency blanket mode reconstructions (See Ref. [12])

Frequency [Hz]	Mode Shape Description	
0.61	1st structural torsion and right blanket edge flap	
0.66	1st structural torsion and right blanket edge flap	
0.78	Left blanket edge flapping	

American Institute of Aeronautics and Astronautics

V. Preliminary Finite Element Calibration

As with the ground vibration tests, the finite element models for the flight configuration of ROSA over-predicted the first bending mode. One critical difference between these two situations is that visual evidence and torque readings in the SPDM suggest that the base of ROSA on ISS may not have been as steady as was anticipated. Adding to the evidence that the boundary conditions of ROSA were softer than expected was the fact that the first bending mode was so hard to excite on the ISS after being easily excited by sine sweeps of smaller amplitude on the ground. It seems likely that ROSA was interacting with the structural dynamics of the SPDM. The exact nature of this interaction is hard to judge without finite element models of the SPDM however.

The uneven blanket modes are a more tractable model calibration problem to tackle. After flight, a number of modifications were made to the Abaqus FEM in an attempt to explain some of the discrepancies between its predictions and measurements taken in flight (see Table 8.) First, material properties were updated to use measured values instead of those used in preflight predictions and based on manufacturer specifications and classical lamination theory. This change lowered overall frequencies but led to no other substantial changes.
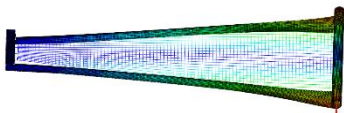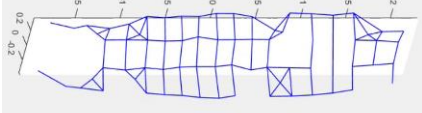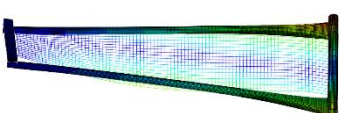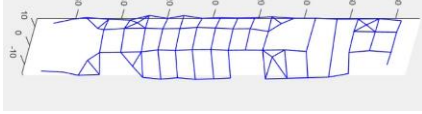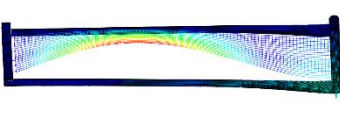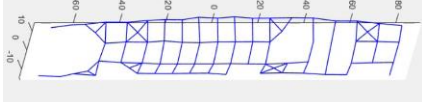
Next, a series of models were created to explore the hypothesis that uneven tensioning in the four constant force springs that applied force to the blanket could explain the separation of IMBA modes in flight. With the tension on the right edge lowered by 50%, very little change was seen in model predictions. After some iteration, it was found that either reducing the tension on the two right-hand side blanket tension springs to nearly zero or tapering the applied tension down to nearly zero on the right created an uneven right blanket edge flapping mode at 0.59 Hz similar to that seen on orbit (see Table 9). The limitations of the Abaqus model are still present however, as the higher frequency modes and separate left blanket edge modes seen on orbit are not produced.

Table 8   Model calibration studies for Abaqus FEM

Mode	Measured Frequency (Hz)	Preflight Model Frequency (Hz)	Postflight Models Frequency (Hz)			
			Adjusted Material Properties	Tension Tapered to 50% Nominal on Right	Tension Tapered to 1N on Right	No Right Side Tension
Structural Bending	0.41	0.50	0.47	0.47	0.46	0.46
Structural twist and right edge flap	0.60	0.64 *	0.60 *	0.60 *	0.59	0.59
Structural twist and right edge flap	0.65	0.98 **	1.00 **	0.88 **	0.70	0.69
* Model predicted a structural torsion mode here						
** Model predicted a blanket bending mode here						

Table 9   Comparison of selected blanket mode shapes pre/post calibration for Abaqus FEM

Mode Shape from Original Preflight FEM with Uniform Blanket Tension	Mode Shape Reconstructed from LaRC Photogrammetry Data	Mode Shape from Calibrated FEM with Blanket Tension Tapered to 1N on Right
0.60 Hz – 1st structural torsion	0.61 Hz - Structural torsion & right blanket edge flap	0.59 Hz – Structural torsion
No Equivalent Mode Predicted	0.66 Hz - Structural torsion & right blanket edge flap	0.70 Hz –Right blanket edge flap
No Equivalent Mode Predicted	0.78 Hz - Left blanket edge flapping	*No Equivalent Mode Predicted*

American Institute of Aeronautics and Astronautics

As further data from the flight test becomes available, model calibration efforts will continue with an eye towards:
1. Explaining the particular structural dynamics of ROSA as measured on-orbit;
2. Showing where differences between these two modeling approaches had the greatest impact on accurate predictions; and
3. Improving future efforts to model lightweight solar array structures and high-strain composite structures like ROSA.

VI. Discussion

The two-headed effort to model and predict the structural dynamics of the ROSA flight experiment on the International Space Station has been described in this paper. Separate government and contractor teams worked in parallel to build finite element models of ROSA in order to predict ground dynamics test results and flight test results. Using different software, assumptions, and overall approaches, the two teams built models that generated similar results for the basic structural modes of the solar array. While both modeling approaches served well in predicting ground test results, unexpected phenomena seen in flight testing created modes and mode shapes not predicted even in sensitivity studies prior to flight.

The point in creating two separate models of ROSA with different approaches and assumptions was to gather two truly independent predictions of its structural dynamics. Each approach had advantages but the Ansys model –by virtue of its experimentally-validated shell model of the blanket- provided a much more comprehensive picture of the dynamics of the IMBA. The Abaqus model included explicit representation of how the boom was flattened onto the mandrel but the beam-based IMBA representation it included could not predict most of the blanket modes. The Abaqus approach also suffered from the need to reimport the results of the explicit boom rolling simulation into the implicit model of the whole array assembly. In the end, however, both models produced booms with transition shapes that qualitatively appeared to accurately model the flight configuration. They also produced accurate mass values for the array. Finally, both models made similar predictions for the first structural modes and blanket modes of the solar array, lending confidence to the planning for in-flight experimentation. During flight, the models provided a valuable tool to assess how the unexpected structural dynamics observed might have come about. Given the accuracy of both models during ground testing and the preliminary results of calibration studies, the authors are confident that they could accurately predict the nominal performance of future ROSA embodiments.

Calibration of the pre-flight models with empirical data gathered in space has just begun and is touched on lightly in the previous section. This calibration is expected to be an ongoing effort as data gleaned from photogrammetry analyses of video recorded during experimentation continues to be generated.

Acknowledgments

American Institute of Aeronautics and Astronautics

References

[1] Banik, J.A., and Hausgen, P., " Roll-Out Solar Arrays (ROSA): Next Generation Flexible Solar Array Technology for DoD Spacecraft," *2017 AIAA SPACE and Astronautics Forum and Exposition*, 12-14 September 2017, Orlando, Florida. AIAA-2017-5307.

[2] Banik, J., Urioste, B., "Chapter 7: Spaceflight Testing," *Testing Large Ultra-Lightweight Spacecraft. AIAA Progress Series in Aeronautics and Astronautics*. Vol 253. 2017. pp. 215-253.

[3] Banik, J., LaPointe, M., Kiefer, S., "On-Orbit Validation of the Roll-Out Solar Array," *IEEE Aerospace 2018 in Big Sky, MT*, 4-11 March 2018. Accepted for Publication.

[4] ASA homepage, International Space Station Research and Technology, Roll Out Solar Array (ROSA) https://www.nasa.gov/mission_pages/station/research/experiments/2139.html Accessed 15 April 2017.

[5] Werner, D., "Market Disruptor", *Aerospace America*, October, pp. 34-38, 2017.

[6] Genna, M., "Innovation: Solar Array Success for SSL Implementation—A Space Systems Loral Focus", *SatMagazine*, September, pp. 104-105, 2017.

[7] Banik, J.A., Kiefer, S.H., LaPointe, M. and P. LaCorte, "On-Orbit validation of the Roll-Out Solar Array," *39th IEEE Aerospace Conference*, 3-10 March 2018, Big Sky, MT.

[8] Spence, B., LaPointe, M., White, S., LaCorte, P., and S. Kiefer, "International Space Station (ISS) ROSA Solar Array Flight Experiment Mission and Results," *36th Annual Space Power Workshop*, 23-25 April 2018, Los Angeles.

[9] Yates, H. and B. Hoang, "SSL ROSA Qualification Status," *36th Annual Space Power Workshop*, 23-25 April 2018, Los Angeles.

[10] Jones, T.W., Liddle, D.A., Shortis, M.R., and J.A. Banik, "On-Orbit Photogrammetry Analysis of the Roll-Out Solar Array (ROSA), accepted for the *6th AIAA Spacecraft Structures Conference, AIAA SciTech Forum*, 7-11 January 2019, San Diego, CA.

[11] Chamberlain, M.K., Kiefer, S.H., and Banik, J.A., "On-Orbit Structural Dynamics Performance of the Roll-Out Solar Array," *5th AIAA Spacecraft Structures Conference, AIAA SciTech Forum*, 8-12 January 2018, Orlando, FL. AIAA-2018-1942.

[12] Chamberlain, M.K., Kiefer, S.H., and Banik, J.A., "Photogrammetry-Based Analysis of the On-orbit Structural Dynamics of the Roll-Out Solar Array," accepted for the *6th AIAA Spacecraft Structures Conference, AIAA SciTech Forum*, 7-11 January 2019, San Diego, CA.

[13] Daniel, I. M., Ishai, O., "Engineering Mechanics of Composite Materials", 2nd ed., Oxford Press, New York, 2006, Chap. 7.

[14] Juang, J.-N., Horta, L.G., and Phan, M.: "System/Observer/Controller Identification Toolbox from Input/Output Measurement Data." User's Guide, NASA TM-107566, 1992.

[15] Horta, L.G., Juang, J-N, and Chen, C.-W.: "Frequency Domain Identification Toolbox." NASA TM-109039, 1996.

American Institute of Aeronautics and Astronautics